THERMAL APPLICATIONS OF CARBON NANOTUBES (SWCNTs-MWCNTs) DUE TO ACCELERATING PLATE WITH RAMPED TEMPERATURE CONDITIONS: ADVANCED FRACTIONAL SIMULATIONS

KAOUTHER GHACHEM[1], SAMI ULLAH KHAN[2,*], IMEN SAFRA[1], HIND ALBALAWI[3], BADR M. ALSHAMMARI[4], LIOUA KOLSI[5]

[1]Department of Industrial and Systems Engineering, College of Engineering, Princess Nourah bint Abdulrahman University, P.O. Box 84428, Riyadh 11671, Saudi Arabia, imsafra@pnu.edu.sa, kgmaatki@pnu.edu.sa

[2,*]Department of Mathematics, Namal University, Mianwali 42250, Pakistan sk_iiu@yahoo.com

[3]Department of Physics, College of Sciences, Princess Nourah bint Abdulrahman University, P.O. Box 84428, Riyadh, 11671, Saudi Arabia, hmalbalawi@pnu.edu.sa

[4]Department of Electrical Engineering, College of Engineering, University of Ha'il, Ha'il City, 81451, Saudi Arabia bms.alshammari@uoh.edu.sa

[5]Department of Mechanical Engineering, College of Engineering, University of Ha'il, Ha'il City, Saudi Arabia, lioua_enim@yahoo.fr

[*]Correspondence: sk_iiu@yahoo.com

Abstract: *The fractional models have emerged as powerful tools for analyzing the behavior of complex systems with applications of memory effects, nonlocality and hereditary consequences. The fractional models offer excellent accuracy between experimental and theoretical results across different physical, thermal, industrial and biological problems. In current analysis, a fractional model has been developed for analyzing the thermal impact of hybrid nanofluid with enhanced heat transfer features. A suspension of water and human blood with carbon nanotubes has been considered. The thermal discretization of hybrid model is attributed with utilization of single wall carbon nanotubes (SWCNT) and multi wall carbon nanotubes (MWCNTs). An accelerating porous plate induces the flow. The problem is further updated by utilizing the magnetic force effects, porosity medium and ramped temperature constraints. Ramped thermal constraints at different time instant are considered. The fractional simulations are performed with help of Prabhakar fractional approach. Comparative thermal results for SWCNT-MWCNT/blood and SWCNT-MWCNT/H_2O have been prepared. The physical insight of parameters in fluctuating the heat transfer rate is observed. The comparative outcomes reveal that water-based CNTs demonstrate a stronger thermal response than blood-based suspension. It has been observed that Grashof number plays effective role in enhancing the heat transfer impact. Presence of porous medium increase the thermal profile, justifying applications in petroleum engineering and soil sciences. The claimed results present novel applications in heat transfer systems, extrusion processes, energy-efficient chemical engineering operations, heat transfer devices, extrusion processes, energy growth, solar systems, chemical processes, fission reactions etc.*

Keywords: Fractional model, heat transfer, hybrid nanofluid; magnetic force; oscillating plate.

1. Introduction

Recent advancements in nanotechnology have engaged significant applications of nanomaterials in renewable systems and thermal management systems. The nanofluids exhibit superior thermal properties and stable mechanical properties as compared to conventional base liquids. The primarily mechanisms contributes to boosted thermal impact include thermophoretic motion, Brownian diffusion and liquid layering around the particles. Various applications of nanofluids are observed in recent days including cooling of various electronic devices, automotive engineering, aerospace thermal systems, solar collectors, chemical and nuclear reactors etc. The contribution of nanomaterials is also observed in medical sciences like drug delivery systems, medical imagining and hyperthermia treatment. The pioneer investigation disclosing thermal aspects of nanofluid was claimed by Choi [1]. Salhi et al. [2] focused to evaluation of heat transfer due to nanofluid in wavy channel. Reddy et al. [3] explored the heat transfer effects due to micropolar fluid with suspension of magnesium oxide nanoparticles. Hassan et al. [4] discussed the role of variable viscosity in thermal aspects of nanofluid under the assumptions of high shear constraints. Waini et al. [5] examined the thermal onset of various nanoparticles in porous medium subject to mixed convection phenomenon. The study exploring the free convection flow of nanofluid in a porous medium was conducted by Babazadeh et al. [6]. Asadi et al. [7] proposed the thermal influence and stability of titanium dioxide and copper nanoparticles for consideration of heat transfer impact. Dhif et al. [8] focused to applications of nanomaterials in solar collectors. Huminic et al. [9] predicted various thermal structures subject to physical conditions and entropy generation due to nanofluids. Nadeem et al. [10] studied the thermal characteristics of nanofluid associated to exponentially curved surface. Song et al. [11] examined Marangoni convection in hybrid nanofluid by entertaining additional heating source. Shoaib et al. [12] investigated the applications of ohmic dissipation in nanofluid flow with optimized performances. The behavior of Williamson nanofluid around a stretched cylinder, influenced by mixed convection, was focused by Song et al. [13]. Kumar et al. [14] analyzed the dynamics of dust particles in the presence of hybrid nanoparticles by employing a modified heat flux approach. Gowda et al. [15] applied Stefan thermal constraints to evaluate the heat transfer characteristics due to Sutterby nanofluid. Prasannakumara [16] responded the influence of magnetic dipoles in Maxwell nanofluid flow accurse a stretched surface. Nagapavani et al. [17] claimed thermal effects in study of heat transfer in presence of various nanoparticles. Mahanthesh's [18] determines the hybrid nanofluid thermal evaluation by entertaining water and ethylene glycol as a base fluid. Acharya [19] predicted the thermal behavior of hybrid nanoparticles through micro-wavy channel. Mackolil and Mahanthesh [20] pointed out the thermal dynamics of Casson nanofluid with impact of thermal radiation. Acharya [21] depicted the hybrid nanofluid thermal prospective for buoyancy driven flow confined by annular enclosure. Acharya et al. [22] predicted the entropy generation in hybrid nanofluid in annular enclosure.

Carbon nanotubes (CNTs) is made of carbon atoms organized in hexagonal lattice with cylindrical nanostructures. Subject to more stable mechanical and electrical properties, the carbon nanotubes are highly involved in nanotechnology, energy systems and materials sciences. The CNTs are further characterized into single-walled carbon nanotubes (SWCNTs) and multi-walled carbon nanotubes (MWCNTs). The SWCNTs consisting of single graphene sheet rolled into tube while the structure of MWCNTs is represented via multiple concentric graphene cylinders. The significance of SWCNTs and MWCNTs is

observed in sensors, transistors, energy storage systems, polymer and metals, super-conductors, fuel cells, drug delivery etc. Acharya et al. [22] observed the buoyancy flow of carbon nanotubes in circular chamber. Mahmood et al. [23] address the slip flow of carbon nanotubes by using the Yamada-Ota model. Farooq et al. [24] explained the contribution of bioconvection while addressing the thermal impact due to carbon nanotubes. Thermal evaluation due to SWCNTs and MWCNTs for rotating flow has been identified by Khan et al. [25].

Fractional models have engaged as powerful tools in mathematical modelling due memory effects and hereditary features inherent in various physical and engineering systems. In category of fractional models, the Caputo, Caputo-Fabrizio and Atangana-Baleanu are famous fractional tools with diverse kernel functions [26-28]. Prabhakar model is also famous fractional technique which has been implemented in various physical models. The motivations for implementing the Prabhakar model are associated to non-local behavior, memory features and hereditary features inherent in various complex fluid and thermal systems. Unlike traditional integral order models, the Prabhakar model provides more impressive and generalized framework by combining various parameters like order and kernel which collectively presents greater flexibility in physical systems. This model provides modified definitions to different fractional operators like Caputo, Caputo-Fabrizio and Atangana-Baleanu tools. Various mathematical models have been presented by using Prabhakar derivatives [29-34].

Mixed convection phenomenon refers to simultaneous appearance of free convection and forced convective within flow system, where buoyancy forces and external forces contribute to heat and momentum transport. The significance of mixed convection is observed in cooling and heating of vertical surfaces, thermal collectors, nuclear systems, electron devices. The thermal behavior and fluid nature in such systems are impacted by interplay between the buoyancy and inertial forces. Haris et al. [35] studied the mixed convection flow for dual cavity with implementation of lattice Boltzmann technique. Hussein et al. [36] presented a research review on significance of mixed convection in trapezoidal enclosures. Investigation for mixed convection in cubic cavity, comprising the hybrid nanofluid was visualized by Bahoum et al. [37]. Khan et al. [38] responded the Ohmic dissipation in mixed convection flow of hybrid nanofluid via computational approach.

1.1 Proposed fractional model

The motivated research presents a novel fractional model for buoyancy driven flow of carbon nanotubes (CNTs) due to inclined oscillating plate. A uniform suspension of single wall carbon nanotubes (SWCNT) and multi wall carbon nanotubes (MWCNTs) with blood and water is considered to inspects the heat transfer phenomenon. A natural convective flow of CNTs has been studied with applications of magnetic force effects and mixed convection applications. The ramped temperature at various flow instants is taken into observations. The impact of porous space and magnetic force along inclined direction is presented. The interesting aspect of current analysis is the implementation of new fractional technique namely Prabhakar fractional scheme. The Prabhakar fractional model was introduced by Prabhakar in 1971. This fractional model contains more generalized Mittag-Leffler function as compared to other fractional algorithms. Moreover, this scheme successfully treated the issue of local and non-local kernels. It is remarked that the observations based on current hybrid nanofluid model can report applications in the thermal industry and

engineering systems. Moreover, the implementation of new Prabhakar fractional model can direct the researchers to implement it for many other physical and scientific problems.

1.2. Research gap and novelty of work

Despite the increasing attention in nanomaterials for thermal and biomedical applications, available investigations have primarily concentrated on the conventional nanofluids in base materials with standard flow constraints. Very few studies have addressed the magnetized flow of hybrid carbon nanotubes, particularly with suspension of human blood and water which are relevant to biomedical and engineering systems. The objective of current analysis to develop a fractional model for carbon nanotubes (CNTs) containing both single wall carbon nanotubes (SWCNT) and multi wall carbon nanotubes (MWCNTs) with blood and water base liquid. The source of flow is porous oscillating plate. A nonlinear model is used which captures the both viscous and elastic features with complex rheology. The fractional simulations are performed with applications of Prabhakar fractional derivatives, which precisely scrutinize the memory and hereditary features. The implementation of such advanced fractional tool is interesting and remains underexplored in such complex flow scenarios. Furthermore, the thermal problem is tackled with ramped thermal constraints. The existing literature also lacks a thorough exploration of such SWCNTs and MWCNTs suspensions with blood and water base liquids associated to accelerating porous plates flow with ramped temperature boundary conditions, which are more realistic for applications involving biological tissues, energy systems, and porous media. This investigation aims to address such gaps by developing a comprehensive model that integrates all these critical physical aspects to provide new insights into heat and momentum transport in hybrid nanofluid systems.

2. Problem description

In current flow model, the thermal control of carbon nanotubes (CNTs) is observed due to inclined surface. The enhancement in thermal impact of water and blood has been focused by utilizing the single wall carbon nanotubes (SWCNT) and multi wall carbon nanotubes (MWCNTs). An oscillation flow of carbon nanotubes is associated to inclined surface. The nature of flow is time dependent.

In order formulate the governing equations, following assumptions have been followed:

- An unsteady mixed convection flow of single wall carbon nanotubes (SWCNT) and multi wall carbon nanotubes (MWCNTs) with suspension of water and blood base fluids have been considered.
- The inclined oscillating plate induced the flow for $t > 0$. Let $U_o H(t) Cos(\omega t)$ be oscillation velocity with amplitude U_o.
- The velocity component is denoted with $w(y,t)$.
- The magnetic force impact is suggested in inclined direction and results for induced magnetic force are not entertained under low magnetic Reynold number approach.
- It has been assumed that the interaction between fluid particles is small so that Joule heating effects have been neglected.

Following such assumptions, the equations for governing model are presented as [34]:

$$\rho_{nf}\left(\frac{\partial w_{(y,t)}}{\partial t} + \beta^* w(y,t)\right) = \mu_{nf}\frac{\partial^2 w_{(y,t)}}{\partial y^2} + g(\rho\beta_T)_{nf} Cos(\theta_2) T_{(y,t)} - g(\rho\beta_T)_{nf} Cos(\theta_2) T_\infty(\delta) - \frac{\mu_{nf}\varphi}{K} w(y,t) - \sigma_{nf} B_o^2 Sin(\theta_1) w(y,t) \quad (1)$$

$$\left(\rho C_p\right)_{nf}\frac{\partial T_{(y,t)}}{\partial t}=-\frac{\partial \delta_{(y,t)}}{\partial y}, \tag{2}$$

$$\delta_{(y,t)}=-k_{nf}\frac{\partial T_{(y,t)}}{\partial y}. \tag{3}$$

with:

$$w_{(y,0)}=0, \qquad T_{(y,0)}=T_\infty \qquad ; \qquad \forall y\geq 0$$

$$w_{(0,t)}-\mathrm{h}\frac{\partial w}{\partial y}\Big|_{y=0}=U_oH(t)Cos(\omega t), \qquad T_{(0,t)}=\begin{cases}T_\infty+(T_w-T_\infty)\dfrac{t}{t_o}, & 0\leq t\leq t_o\\ T_w, & t>t_o\end{cases}$$

$$w_{(y,t)}\to 0,\ T_{(y,t)}\to T_\infty \quad ; \quad y\to\infty\ ,\ t>0.$$

It has been remarked that boundary constraints for velocity represents oscillatory nature of inclined plate and raped thermal conditions have followed to inspect the thermal profile. Various physical phenomena involve such constraints like rotating machinery, nano-scale thermal actuators, thermal management systems, extrusion processes, food technologies, processing systems and biomedical devices.

The nonlinear flow model (1) is converted into traditional viscous model when $\beta^*=0$.

The new variables are [34]:

$$w^*=\frac{w}{U_o}, \qquad y^*=\frac{U_o}{\upsilon_f}y, \qquad t^*=\frac{U_o^2}{\upsilon_f}t, \qquad T^*=\frac{T_{(y,t)}-T_\infty}{T_w-T_\infty}, \quad q^*=\frac{q}{q_o}$$

$$f(t^*)=f\left(\frac{U_o^2t}{\upsilon_f}\right),\ Pr=\left(\frac{\mu C_p}{\kappa}\right)_f, Gr=\frac{g(\rho\beta_T)_f(T_w-T_\infty)}{U_o^3}, \qquad \beta_1^*=\frac{\upsilon_f}{U_o^2}\beta_1$$

Following above variables, the dimensionless system is:

$$\frac{\partial w_{(y,t)}}{\partial t}+\beta_1 w_{(y,t)}=\frac{1}{\Pi_o\Pi_1}\frac{\partial^2 w_{(y,t)}}{\partial y^2}+\frac{\Pi_2}{\Pi_o}GrT_{(y,t)}Cos(\theta_2)-\left(\mathrm{K}_p+\frac{1}{\Pi_1}\mathrm{M}Sin(\theta_1)\right)w(y,t) \tag{4}$$

$$\Pi_3 Pr\frac{\partial T_{(y,t)}}{\partial t}=-\frac{\partial \delta_{(y,t)}}{\partial y}, \tag{5}$$

$$\delta_{(y,t)}=-\Pi_4\frac{\partial T_{(y,t)}}{\partial y}. \tag{6}$$

with:

$$w_{(y,0)}=0, \qquad T_{(y,0)}=0 \qquad ; \qquad \forall y\geq 0 \tag{7}$$

$$w_{(0,t)}-\mathrm{h}\frac{\partial w}{\partial y}\Big|_{y=0}=H(t)Cos(\omega t)\ , \quad T_{(0,t)}=\begin{cases}t, & 0<t\leq 1\\ 1, & t>1\end{cases} \tag{8}$$

$$w_{(y,t)}\to 0,\ T_{(y,t)}\to 0 \quad ; \quad y\to\infty\ ,\ t>0 \tag{9}$$

In order to present the thermal properties of base liquids along with hybrid nanofluids table 1 has been presented. Table 2 justifies numerical values of hybrid nanofluid.

Table 1: Mathematical expressions for hybrid nanofluid [21, 22, 34].

Physical properties	Mathematical representations
Density	$\rho_f=(1-\varphi)\rho_f+\varphi\rho_s$
Energetic Viscosity	$\mu_{nf}=\mu_f/(1-\varphi)^{5/2}$
Electrical conductivity	$\rho_{nf}/\rho_f=1+3\left(\sigma_s/\sigma_f-1\right)\sigma/\left(\sigma_s/\sigma_f+2\right)\sigma-\left(\sigma_s/\sigma_f-1\right)\sigma$
Heat conductivity	$\kappa_{nf}/\kappa_f=\kappa_s+2\kappa_f-2\varphi\left(\kappa_s-\kappa_f\right)/\kappa_s+2\kappa_f+\varphi\left(\kappa_s-\kappa_f\right)$

Temperature capacitance	$(\rho C_{\mathcal{P}})_{nf} = (1-\varphi)(\rho C_{\mathcal{P}})_f + \varphi(\rho C_{\mathcal{P}})_s$
Thermal Expansion Factor	$(\rho B_T)_{nf} = (1-\varphi)(\rho B_T)_f + \varphi(\rho B_T)_s$

Table 2: Numerical values for base fluids and nanoparticles [19, 21].

Physical quantities	$Blood$	Water	$SWCNTs$	$MWCNTs$
$\rho(kg/m^3)$	1053	997.1	2600	1600
$C_\rho(J/kgK)$	3594	4179	425	796
$k(W/mK)$	0.492	0.613	6600	3000

3. Prabhakar fractional model

Prabhakar fractional model is selected to perform analytical simulations of the problem. The choice of Prabhakar model is subject to its capability of memory features. The understanding of such memory features are predicted through three parameter Mittag-Leffler kernel. This fractional tool is more flexible as compared to other fractional schemes like AB and CF. Prabhakar model is effective for analyzing the anomalous transport phenomena, multi-scale flows, thermal prediction of nanomaterials and various bioengineering applications.

Following the extended form of Fourier theory, the Prabhakar derivative is given by:

$$\delta_{(y,t)} = -\Pi_4\, {}^{C}\mathfrak{D}^{\gamma}_{\alpha,\beta,\alpha}\frac{\partial T_{(y,t)}}{\partial y} \tag{10}$$

where ${}^{C}\mathfrak{D}^{\gamma}_{\alpha,\beta,\alpha}$ be Prabhakar derivative which has been given below [29-31]:

$$\begin{aligned} {}^{C}\mathfrak{D}^{\gamma}_{\alpha,\beta,\alpha}h(t) &= E^{-\gamma}_{\alpha,n,-\beta,\alpha}h^n(t) = e^{-\gamma}_{\alpha,n,-\beta}(\alpha;t) * h^n(t) \\ &= \int_0^t (t-\tau)^{n-\beta-1}\, E^{-\gamma}_{\alpha,n,-\beta}(\alpha(t-\tau)^{\alpha})h^n(\tau)\, d\tau \end{aligned}$$

Now definition of $E^{\gamma}_{\alpha,\beta,\alpha}h(t)$ leads to:

$$E^{\gamma}_{\alpha,\beta,\alpha}h(t) = \int_0^t (t-\tau)^{\beta-1}\, E^{-\gamma}_{\alpha,\beta}(\alpha(t-\tau)^{\alpha})h(\tau)\, d\tau$$

where

$$E^{\gamma}_{\alpha,\beta}(z) = \sum_{m=0}^{\infty}\frac{\Gamma(\gamma+m)z^m}{m!\ \Gamma(\gamma)\Gamma(\alpha m+\beta)}$$

where $e^{\gamma}_{\alpha,\beta}(\alpha;t) = t^{\beta-1}E^{\gamma}_{\alpha,\beta}(\alpha t^{\alpha})$ be Prabhakar kernel. Defining Laplace transform of ${}^{C}\mathfrak{D}^{\gamma}_{\alpha,\beta,\alpha}$ as:

$$\begin{aligned} \mathcal{L}\left[{}^{C}\mathfrak{D}^{\gamma}_{\alpha,\beta,\alpha}\mathrm{h}(t)\right] &= \mathcal{L}\left[h^m(t) * e^{-\gamma}_{\alpha,m-\beta}(\alpha;t)\right] = \mathcal{L}\{h^m(t)\}\mathcal{L}\left\{e^{-\gamma}_{\alpha,m-\beta}(\alpha;t)\right\} \\ &= \mathcal{L}\{h^m(t)\}s^{\beta-m}(1-\alpha s^{-\alpha})^{\gamma} \end{aligned} \tag{11}$$

Above model is deduced into Fourier results when $\beta = \gamma = 0$.

3.1. Simulations for temperature profile

The implementation of Laplace technique on Eqs. (5-10) yield:

$$\Pi_3\,\mathrm{Pr}\,s\,\bar{T}_{(y,s)} = -\frac{\partial\bar{\delta}_{(y,s)}}{\partial y} \tag{12}$$

$$\bar{\delta}_{(y,s)} = -\Pi_4\left(s^{\beta}(1-\alpha s^{-\alpha})^{\gamma}\right)\frac{\partial\bar{T}_{(y,s)}}{\partial y} \tag{13}$$

$$\bar{T}_{(y,s)} = \frac{1-e^{-s}}{s^2}; \qquad \bar{T}_{(y,s)} \to 0, \;\; y \to \infty \tag{14}$$

with

$$\frac{\partial^2 \bar{T}_{(y,s)}}{\partial y^2} - \frac{\Pi_3 \, Pr \, s}{\Pi_3 \, s^{\beta}(1-\alpha s^{-\alpha})^{\gamma}} \bar{T}_{(y,s)} = 0 \tag{15}$$

Following Eq. (14) in Eq. (15) give:

$$\overline{T}_{(y,s)} = \frac{1-e^{-s}}{s^2} e^{-y\sqrt{\frac{\Pi_3 \, Pr \, s}{\Pi_3 \, s^{\beta}(1-\alpha s^{-\alpha})^{\gamma}}}} \tag{16}$$

3.2 Limiting case for Fourier Law

By utilizing Eq. (11), It's clear that

$$\mathcal{L}\left[e^{-\gamma}_{\alpha,\beta}(\alpha;t)\right] = \mathcal{L}\left\{t^{\beta-1}e^{-\gamma}_{\alpha,\beta}(\alpha t^{\alpha})\right\} = s^{\beta}(1-\alpha s^{-\alpha})^{\gamma} \tag{17}$$

For case $\beta = \gamma = 0$, Eq. (17) yields:

$$\mathcal{L}\left[e^{0}_{\alpha,0}(\alpha;t)\right] = 1 = \delta(t)$$

The result for temperature profile are:

$$\overline{T}_{(y,s)} = \frac{1-e^{-s}}{s^2} e^{-y\sqrt{\Pi_3 \, Pr \, s}} \tag{18}$$

with its Laplace inverse

$$T_{(y,t)} = h_1(t) * h_2(t)$$

$$h_1(t) = \mathcal{L}^{-1}\left\{\frac{1-e^{-s}}{s}\right\} = 1 - H(t-1)$$

$$h_2(t) = \mathcal{L}^{-1}\left\{\frac{e^{-y\sqrt{\Pi_3 \, Pr \, s}}}{s}\right\} = \frac{exp\left[-\frac{\Pi_3 \, \mathrm{Pr} \, y^2}{4t}\right] y\sqrt{\Pi_3 \mathrm{Pr} \, t}}{2\sqrt{\pi}\, t}$$

3.3. Simulations for velocity profile

After entertaining the Laplace definition on Eq. (4), one gets:

$$s\,\overline{w}_{(y,s)} + \beta_1 \overline{w}_{(y,s)} = \frac{1}{\Pi_o \Pi_1}\frac{\partial^2 \overline{w}_{(y,s)}}{\partial y^2} + \frac{\Pi_2}{\Pi_o} Gr \bar{T}_{(y,s)} Cos(\theta_2) - \left(\mathrm{K}_p + \frac{1}{\Pi_1}\mathrm{M}Sin(\theta_1)\right) w(y,s) \tag{19}$$

$$\overline{w}_{(0,s)} - \mathrm{h}\frac{\partial \overline{w}}{\partial y}\bigg|_{y=0} = \frac{s}{s^2+\omega^2} \quad ; \quad \overline{w}_{(y,s)} \to 0 \quad as \quad y \to \infty$$

The solution in view of (17) is:

$$\overline{v}_{(y,s)} = \frac{1}{1+h\sqrt{\Pi_o(\Omega_6+\Pi_1 s)}}\left[\frac{\Omega_2(1-e^{-s})}{s^2}\frac{1+\mathrm{h}\sqrt{\frac{\Omega_7 \, s}{\Pi_4 s^{\beta}(1-\alpha s^{-\alpha})^{\gamma}}}}{\frac{\Omega_7 \, s}{\Pi_4 s^{\beta}(1-\alpha s^{-\alpha})^{\gamma}} - \Pi_o(\Omega_6+\Pi_1 s)}\right.$$

$$\left. + \frac{s}{s^2+\omega^2}\right] e^{-y\sqrt{\Pi_o(\Omega_6+\Pi_1 s)}} - \frac{\Omega_2(1-e^{-s})}{s^2}\frac{e^{-y\sqrt{\frac{\Omega_7 \, s}{\Pi_4 s^{\beta}(1-\alpha s^{-\alpha})^{\gamma}}}}}{\frac{\Omega_7 \, s}{\Pi_4 s^{\beta}(1-\alpha s^{-\alpha})^{\gamma}} - \Pi_o(\Omega_6+\Pi_1 s)}$$

where

$$\Omega_1 = \Pi_1\Pi_2 \qquad \Omega_2 = \Omega_1 \, Gr \, Cos(\theta_2), \quad \Omega_3 = \Pi_1\beta_1$$
$$\Omega_4 = \Pi_1 \mathrm{K}_{eff}, \qquad \Omega_5 = \Omega_4 + \mathrm{M}Sin(\theta_1)$$

$$\Omega_6 = \Omega_4 + \Omega_5, \quad \Omega_7 = \Pi_3 Pr$$

. The mathematical forms of both schemes can be distinct as:

$$w(y,t) = \frac{ln(2)}{t}\sum_{n=1}^{N} v_n \overline{w}\left(y, n\frac{ln(2)}{t}\right)$$

where N is a positive integer.

$$v_n = (-1)^{n+\frac{N}{2}} \sum_{r=\left\lfloor\frac{q+1}{2}\right\rfloor}^{min\left(q,\frac{N}{2}\right)} \frac{r^{\frac{N}{2}}(2r)!}{\left(\frac{N}{2}-r\right)!\, r!\ (r-1)!\ (q-r)!\ (2r-q)!}$$

and

$$w(\xi,t) = \frac{e^{4.7}}{t}\left[\frac{1}{2}\overline{w}\left(r,\frac{4.7}{t}\right) + Re\left\{\sum_{j=1}^{N}(-1)^k \overline{w}\left(r,\frac{4.7+k\pi i}{t}\right)\right\}\right]$$

The fractional model is verified via numerical computations in table 3. Table 3 presents comparative analysis of results with investigation of Khan et al. [40]. A fine agreement is observed between both studies.

Table 3: Comparison of results for velocity profile $w(y,t)$ with analysis of Khan et al. [40].

y	Khan et al. [40]	Current results	CPU Time(sec)
0.1	0.8608	0.8610	2.54
0.5	1.0424	1.0426	3.83
0.7	0.9392	0.9393	7.72
1.1	0.6633	0.6635	10.55
1.5	0.4398	0.4399	11.75

4. Results and discussion

Physical interpretation and significance of results is graphically predicted against different flow parameters. The graphical simulations are performed comparatively for water-based single wall carbon nanotubes ($SWCNTs - MWCNTs/H_2O$) and blood-based multi wall carbon nanotubes ($SWCNTs - MWCNTs/blood$). Fig. 1 explores the evaluation of temperature profile $T(y,t)$ due to Hartmann number M. With increasing M, the thermal profile grows gradually. The improvement in temperature profile is larger for $SWCNTs - MWCNTs/H_2O$. Physically, such improvement in heat transfer is associated to applications of Lorentz force. Fig. 2 explores the change in temperature profile $T(y,t)$ due to higher Prandtl number Pr. A declining change in assessment of $T(y,t)$ has been examined for larger values of Pr. The physical aspects behind control of $T(y,t)$ is justified due to smaller thermal diffusivity against higher Pr. Furthermore, the control of temperature rate is relatively slower for $SWCNTs - MWCNTs/H_2O$. In order to check the importance of Grashof number Gr on $T(y,t)$, Fig. 3 has been plotted. It is noticed that , upon increasing Gr, the transfer of heat grows for both suspensions. Such outcomes are physically associated buoyancy forces. Fig. 4 notifies the results for fractional parameter α on profile of $T(y,t)$. The simulated results showing a reverse trend in profile of $T(y,t)$. In order to observe the effects of porosity parameter K_p on $T(y,t)$, Fig. 5 is plotted. The presence of porous medium boosted the transfer of heat and enriches

temperature profile. The enhancement in temperature rate is more progressive for $SWCNTs - MWCNTs/H_2O$. These observations are important for petroleum engineering and soil sciences.

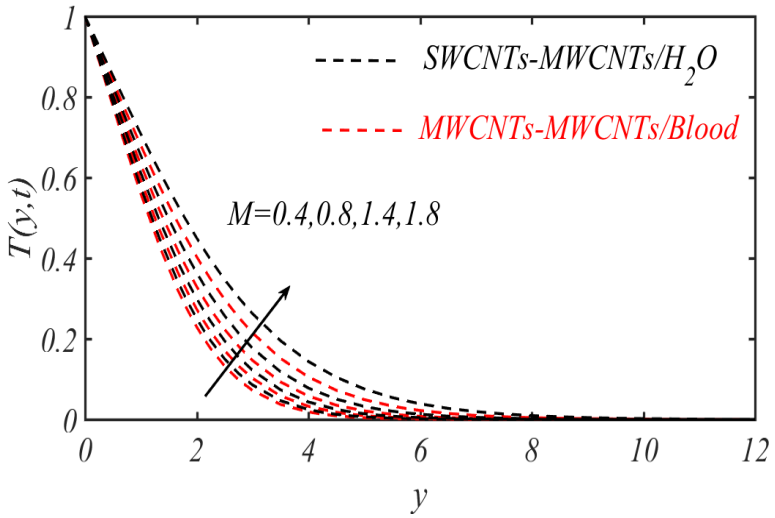

Fig. 1: Variation of temperature for M.

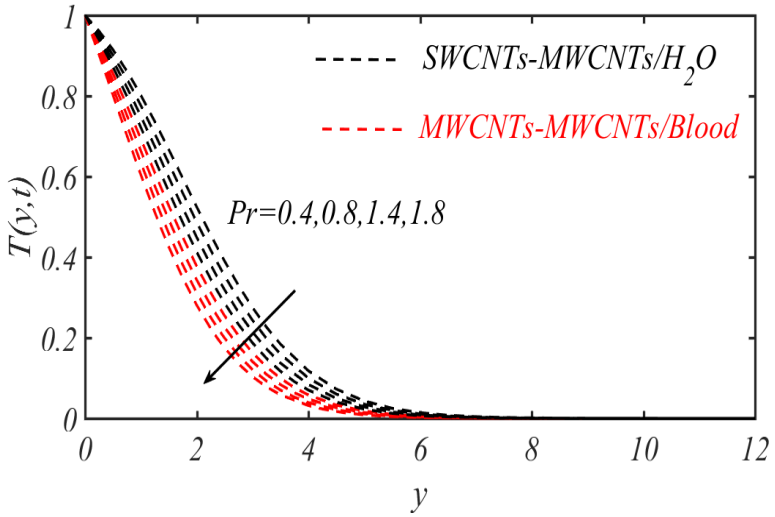

Fig. 2: Variation of temperature for Pr.

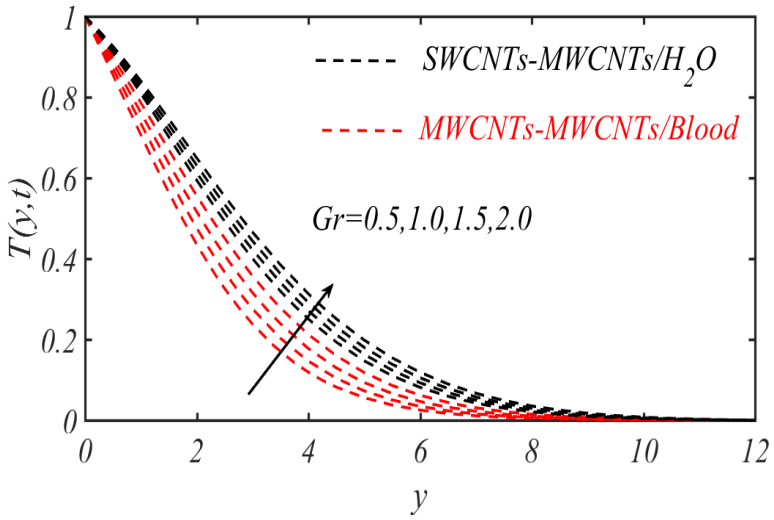

Fig. 3: Variation of temperature for Gr.

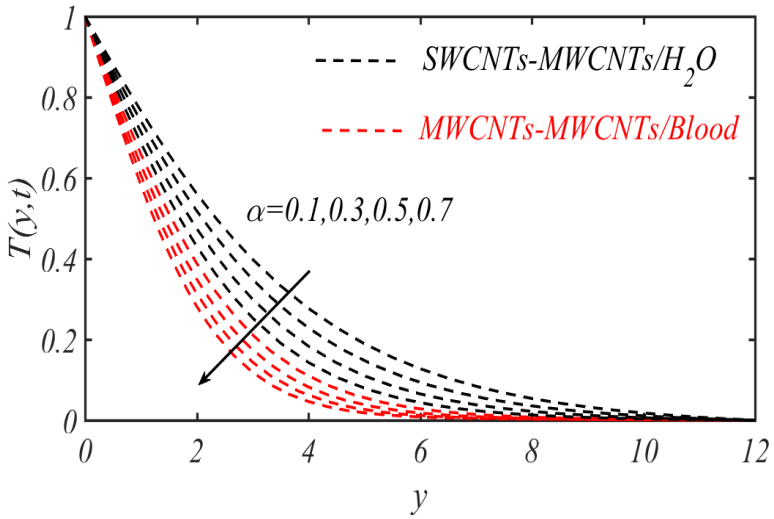

Fig. 4: Variation of temperature for α.

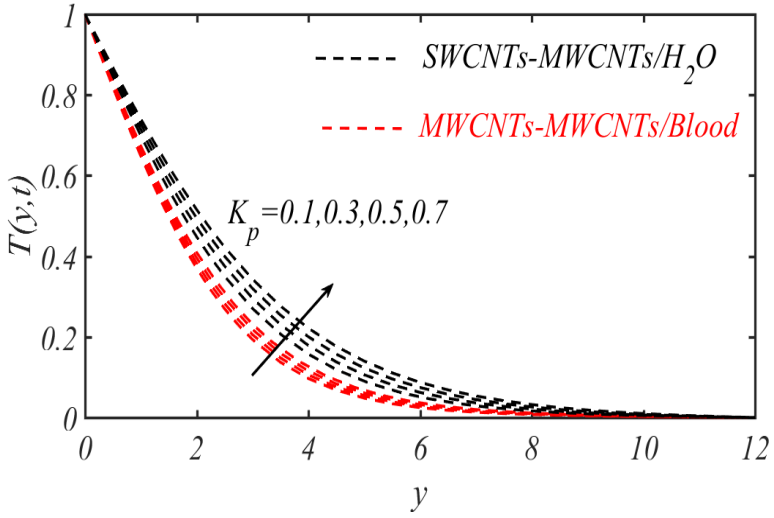

Fig. 5: Variation of temperature for K_p.

Fig. 7 aims to highlight the profile of velocity $w(y,t)$ when the effects of Grashof number Gr are prominent. Physically Gr represents the ratio between buoyancy to viscous forces. Larger Gr enhances the buoyancy forces which leads to be increment of velocity profile. Fig. 8 determines the influence of fractional parameter α on velocity profile $w(y,t)$. Slower change is exhibited in profile of $w(y,t)$ by increasing fractional parameter. Fig. 9 comprises the features of porosity parameter K_p on $w(y,t)$. The resulting results conveying a decrement in velocity due to higher K_p. Physical aspects of such decrement in fluidic velocity is due to permeability of porous media.

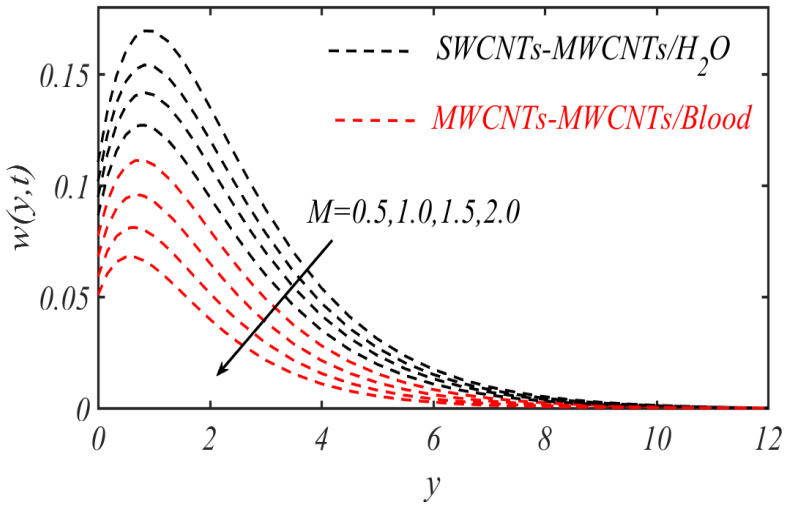

Fig. 6: Variation of velocity for M.

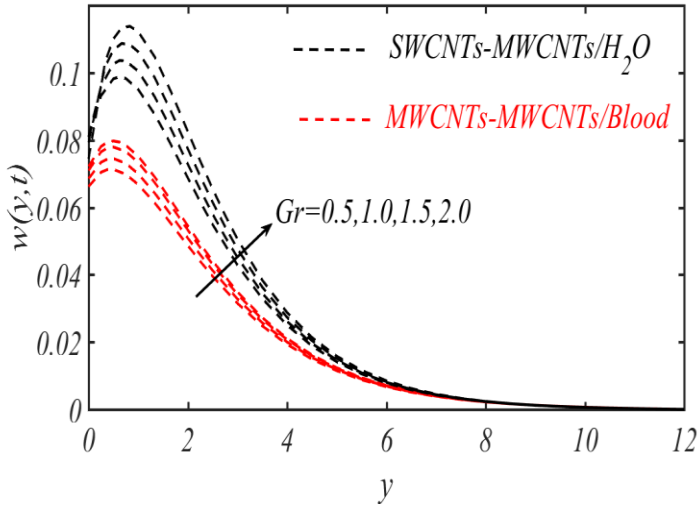

Fig. 7: Variation of velocity for Gr.

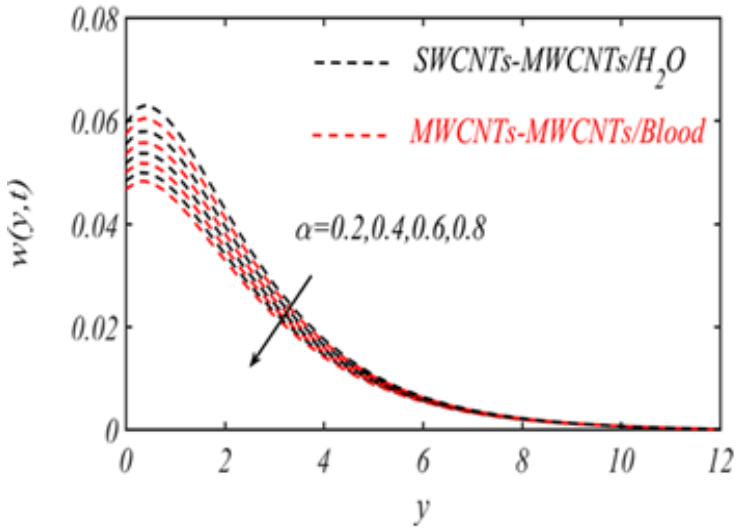

Fig. 8: Variation of velocity for α.

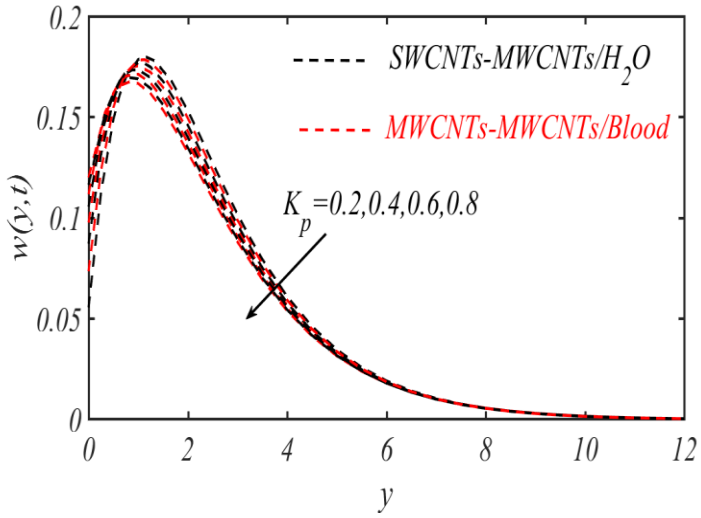

Fig. 9: Variation of velocity for K_p.

5. Conclusions

This investigation presents fractional simulations thermal flow of carbon nanotubes with suspension of human blood and water base liquids. Realistic ramped thermal constraints are used to analyze the thermal phenomenon. The comparative thermal evaluation of model are addressed for $SWCNTs - MWCNTs/H_2O$ and $SWCNTs - MWCNTs/Blood$. The concluded observations are:

- The heat transfer enhances due to Hartmann number subject to applications of Lorentz force. The improvement in heat transfer is more impressive for water-based nanofluid compared to the blood-based carbon nanotubes.
- Higher Prandtl number effectively reduces the temperature field due to low thermal diffusivity. The cooling features are more pronounced for blood based carbon nanotubes.
- An enhancement in temperature and velocity profiles is examined due to higher Grashof number, indicating the significance of buoyancy forces.

- By increasing porosity parameter, the temperature profile increase by fascinating the transfer of heat in porous medium, especially for $SWCNTs - MWCNTs/H_2O$.
- A declining trend in temperature and velocity profiles has been examined due to fractional parameter, comprising the memory effects that controls the thermal transport phenomenon.
- The proposed model provides direction to develop advanced models for various transport phenomena in complex systems like bio-fluids, thermal management systems, flow through porous media, energy systems etc. This model also encourages the future studies on designing efficient numerical schemes and machine learning algorithms.

Acknowledgment:

This research project was funded by the Deanship of Scientific Research and Libraries, Princess Nourah bint Abdulrahman University, through the Program of Research Project Funding After Publication, grant No (RPFAP-111- 1445).

References

[1]. Choi, S. U. S and Eastman, J. A., Enhancing thermal conductivity of fluids with nanoparticles," Argonne National Lab.(ANL), Argonne, IL (United States), 1995.

[2]. Salhi, H., Mohamed S. A., and Haddad, D., Numerical study of natural convection heat transfer performance in an inclined cavity with complex-wavy-wall: nanofluid and random temperature, *Computational Thermal Sciences: An International Journal*, 7(1), (2015) pp 51-64.

[3]. Reddy, M., and Shehzad, S., Molybdenum disulfide and magnesium oxide nanoparticle performance on micropolar Cattaneo-Christov heat flux model, *Applied Mathematics and Mechanics*, vol. 42(4), (2021) pp. 541-552.

[4]. Hassan, M., Oudina, F. M., Faisal, A., Ghafar, A., and Ismail, A. I., Thermal energy and mass transport of shear thinning fluid under effects of low to high shear rate viscosity, *International Journal of Thermofluids*, 15, (2022) pp. 100176.

[5]. Waini, A., Ishak, A., Groşan, T. and Pop, I., Mixed convection of a hybrid nanofluid flow along a vertical surface embedded in a porous medium, *International Communications in Heat and Mass Transfer*, 114, (2020) pp. 104565.

[6]. Babazadeh, H., Shah, Z., Ullah, I., Kumam, P. and Shafee, A., Analysis of hybrid nanofluid behavior within a porous cavity including Lorentz forces and radiation impacts," *Journal of Thermal Analysis and Calorimetry*, vol. 143(2), (2021) pp. 1129-1137.

[7]. Asadi, A., Alarifi, I. M., and Foong, L. K., An experimental study on characterization, stability and dynamic viscosity of CuO-TiO2/water hybrid nanofluid," *Journal of Molecular Liquids*, 307, (2020) pp. 112987.

[8]. Dhif, K., Mebarek-Oudina, F., Chouf, S., Vaidya, H. and Chamkha, A. J., Thermal analysis of the solar collector cum storage system using a hybrid-nanofluids. *Journal of Nanofluids*, *10*(4), (2021) pp. 616-626.

[9]. Huminic, G. and Huminic, A., Entropy generation of nanofluid and hybrid nanofluid flow in thermal systems: a review. *Journal of Molecular Liquids*, *302*, (2020) p.112533.

[10]. Nadeem, S., Abbas, N. and Malik, M.Y., 2020. Inspection of hybrid based nanofluid flow over a curved surface. *Computer methods and programs in biomedicine*, *189*, p.105193.

[11]. Song, Y.Q., Khan, M.I., Qayyum, S., Gowda, R.P., Kumar, R.N., Prasannakumara, B.C., Elmasry, Y. and Chu, Y.M., Physical impact of thermo-diffusion and diffusion-thermo on Marangoni convective flow of hybrid nanofluid (MnZiFe2O4–NiZnFe2O4–H2O) with nonlinear heat source/sink and radiative heat flux. *Modern Physics Letters B*, *35*(22), (2021) p.2141006.

[12]. Shoaib, M., Zubair, G., Nisar, K.S., Raja, M.A.Z., Khan, M.I., Gowda, R.P. and Prasannakumara, B.C., Ohmic heating effects and entropy generation for nanofluidic system of Ree-Eyring fluid: Intelligent computing paradigm. *International Communications in Heat and Mass Transfer*, *129*, (2021) p.105683.

[13]. Song, Y.Q., Hamid, A., Sun, T.C., Khan, M.I., Qayyum, S., Kumar, R.N., Prasannakumara, B.C., Khan, S.U. and Chinram, R., Unsteady mixed convection flow of magneto-Williamson nanofluid due to stretched cylinder with significant non-uniform heat source/sink features. *Alexandria Engineering Journal*, *61*(1), (2022) pp.195-206.

[14]. Varun Kumar, R.S., Punith Gowda, R.J., Naveen Kumar, R., Radhika, M. and Prasannakumara, B.C., Two-phase flow of dusty fluid with suspended hybrid nanoparticles over a stretching cylinder with modified Fourier heat flux. *SN Applied Sciences*,*3*(3), (2021) p.384.

[15]. Gowda, R.P., Kumar, R.N., Rauf, A., Prasannakumara, B.C. and Shehzad, S.A., Magnetized flow of sutterby nanofluid through cattaneo-christov theory of heat diffusion and stefan blowing condition. *Applied Nanoscience*, 13(1), (2023) pp.585-594.

[16]. Prasannakumara, B.C., Numerical simulation of heat transport in Maxwell nanofluid flow over a stretching sheet considering magnetic dipole effect. *Partial Differential Equations in Applied Mathematics*, 4, (2021) p.100064.

[17]. Nagapavani, M., Kanuri, V.R., Fareeduddin, M., Thanesh Kumar, K., Kolli, U.C., Sunitha, M., Gali, C. and Naveen Kumar, R., Features of the exponential form of internal heat generation, Cattaneo–Christov heat theory on water-based graphene–CNT–titanium ternary hybrid nanofluid flow. *Heat Transfer*, 52(1), (2023) pp.144-161.

[18]. Mahanthesh, B., Statistical and exact analysis of MHD flow due to hybrid nanoparticles suspended in C2H6O2-H2O hybrid base fluid. In *Mathematical methods in engineering and applied sciences*, (2020) pp. 185-228.

[19]. Acharya, N., Magnetically driven MWCNT-Fe3O4-water hybrid nanofluidic transport through a micro-wavy channel: a novel MEMS design for drug delivery application. *Materials Today Communications*, 38 (2024) p.107844.

[20]. Mackolil, J., Mahanthesh, B., Exact and statistical computations of radiated flow of nano and Casson fluids under heat and mass flux conditions, *Journal of Computational Design and Engineering*, 6(4), (2019) pp. 593-605

[21]. Acharya, N., Effects of the curved fins on the entropy analysis and hydrothermal variations of Buoyancy-driven MWCNT-Fe3O4-H2O hybrid nanofluid flow within an annular enclosure." *Applied Thermal Engineering*, 269 (2025): p. 126100.

[22]. Acharya, N., Framing the effect of fitted curved fins' curvature on the flow patterns and entropy analysis of buoyancy-driven magnetized hybrid nanofluidic transport within an annular enclosure." *Journal of Energy Storage*, 100 (2024): p. 113638.

[23]. Acharya, N., Hydrothermal scenario of buoyancy-driven magnetized multi-walled carbon nanotube-Fe3O4-water hybrid nanofluid flow within a discretely heated circular chamber fitted with fins." *Journal of Magnetism and Magnetic Materials*, 589 (2024): p. 171612.

[24]. Mahmood, Z., Rafique, K., Adnan, Khan, U., Muhammad, T. and Hassan, A.M., 2024. MHD unsteady flow of carbon nanotubes over nonlinear radiative surface with anisotropic slip conditions: computational analysis of irreversibility for Yamada-Ota model. *Engineering Applications of Computational Fluid Mechanics*, 18(1), p.2309139.

[25]. Farooq, U., Liu, T. and Jan, A., 2025. Boundary layer analysis of second-order magnetic nanofluid flow with carbon nanotubes and gyrotactic microorganisms for medical diagnostics. *BioNanoScience*, 15(1), p.113.

[26]. Khan, S.U., Majeed, A. and Aziz, S., Thermal prediction of rotatory multiwall carbon nanotubes subject to convective boundary conditions and slip effects: Implicit finite difference simulations. *Numerical Heat Transfer, Part B: Fundamentals*, 86(5), (2025) pp.1196-1209.

[27]. Sene, N., 2020. Second-grade fluid model with Caputo–Liouville generalized fractional derivative. *Chaos, Solitons & Fractals*, *133*, p.109631.

[28]. Mozafarifard, M. and Toghraie, D., Time-fractional subdiffusion model for thin metal films under femtosecond laser pulses based on Caputo fractional derivative to examine anomalous diffusion process. *International Journal of Heat and Mass Transfer*, 153, (2020) p.119592.

[29]. Asjad, M.I., Zahid, M., Chu, Y.M. and Baleanu, D., Prabhakar fractional derivative and its applications in the transport phenomena containing nanoparticles. *Thermal Science*, 25(Spec. issue 2), (2021) pp.411-416.

[30]. Sarwar, N., Asjad, M.I., Sitthiwirattham, T., Patanarapeelert, N. and Muhammad, T., A Prabhakar fractional approach for the convection flow of Casson fluid across an oscillating surface based on the generalized Fourier law. *Symmetry*, 13(11), (2021) p.2039.

[31]. Asjad, M.I., Sunthrayuth, P., Ikram, M.D., Muhammad, T. and Alshomrani, A.S., Analysis of non-singular fractional bioconvection and thermal memory with generalized Mittag-Leffler kernel. *Chaos, Solitons & Fractals*, 159, (2022) p.112090.

[32]. Giusti A., and Colombaro, I., Prabhakar-like fractional viscoelasticity, *Communications in Nonlinear Science and Numerical Simulation,* vol. 56 (2018) pp. 138-143.

[33]. A. Akgül and I. Siddique, "Novel applications of the magnetohydrodynamics couple stress fluid flows between two plates with fractal-fractional derivatives," *Numerical Methods for Partial Differential Equations*, vol. 37, no. 3, (2021) pp. 2178-2189.

[34]. Asjad, M.I., Zahid, M., Chu, Y.M. and Baleanu, D., Prabhakar fractional derivative and its applications in the transport phenomena containing nanoparticles. *Thermal Science*, *25*(Spec. issue 2), (2021) pp.411-416.

[35]. Ghachem, K., Javid, K., Ullah, K.S., Safra, I., Albalawi, H. and Kolsi, L., MHD flow and thermal analysis of water-based nanofluids with copper (CU) and aluminum oxide (Al2O3) nanoparticles: An advanced fractional approach. *Thermal Science*, Online First, (2025) https://doi.org/10.2298/TSCI241203069G

[36]. Haris, M., Mixed convection analysis in a dual-driven cavity with a stable vertical temperature gradient using the lattice Boltzmann method. *Thermal Science*, 29, (2025), 3B pp.2277-2296

[37]. Hussein, A.K., Togun, H., Rashid, F.L., Basem, A., Abed, A.M., Al-Obaidi, M.A., Abdulrazzaq, T., Dhabab, J.M., Attia, M.E.H., Ali, B. and Rout, S.K., Mixed convection in trapezoidal enclosures containing mono and hybrid nanofluids: a comprehensive review. *Journal of the Brazilian Society of Mechanical Sciences and Engineering*, *47*(4), (2025) p.176.

[38]. Bahoum, A., El, H.M. and El, H.Y., Numerical investigation of mixed magneto-hydrodynamic convection in a lid-driven cubic cavity with a hybrid nanofluid. *Thermal Science*, 29, (2025) 4A, pp. 2713-2728.

[39]. Khan, M., Qamar, M., Shan, M. and Yasir, M., Thermally mixed convection flow of radiated hybrid nanofluids with Ohmic dissipation and Newtonian heating. *Journal of Radiation Research and Applied Sciences*, 18(2), (2025) p.101344.

[40]. Khan, S. U., Raza, A., Kanwal, A., The inclined surface flow of hybrid nanofluid with Newtonian heating and general velocity flow constraints: the Prabhakar model, *Waves in Random and Complex Media*, 1–12 (2022) https://doi.org/10.1080/17455030.2022.2160031.

Nomenclature

ρ_{nf}	density	β^*	Viscoelastic coefficient
w	Velocity component	t	Time
g	gravity	θ_2	Inclined angle
T_∞	Ambient temperature	φ	Porous Medium
μ_{nf}	Dynamic viscosity	σ_{nf}	Electrical conductivity
$(\rho C_p)_{nf}$	Specific heat	B_0	Magnetic force strength
K	Permeability medium	k_{nf}	Thermal conductivity
T	Temperature	U_o	Surface velocity
ω	Angular frequency	T_w	Convective temperature
Gr	Thermal Grashof number	Pr	Prandtl number

Submitted: 6.6.2025.
Revised: 31.7.2025.
Accepted: 04.08.2025.